

# Contribution of Galaxies to the Background Hydrogen-Ionizing Flux

Julien E. G. Devriendt,<sup>1</sup> Shiv K. Sethi,<sup>1</sup> Bruno Guiderdoni,<sup>1</sup> and Biman B. Nath<sup>2</sup>

<sup>1</sup> Institut d’Astrophysique de Paris, CNRS, 98bis Boulevard Arago F-75014 Paris France

<sup>2</sup> Raman Research Institute, Bangalore-560080, India

28 August 2018

## ABSTRACT

We estimate the evolution of the contribution of galaxies to the cosmic background flux at 912Å by means of a semi-analytic model of galaxy formation and evolution. Such a modelling has been quite successful in reproducing the optical properties of galaxies. We assume hereafter the high-redshift damped Lyman- $\alpha$  (DLA) systems to be the progenitors of present day galaxies, and we design a series of models which are consistent with the evolution of cosmic comoving emissivities in the available near infrared (NIR), optical, ultraviolet (UV), and far infrared (FIR) bands along with the evolution of the neutral hydrogen content and average metallicity of damped Lyman- $\alpha$  systems (DLA). We use these models to compute the galactic contribution to the Lyman-limit emissivity and background flux for  $0 \leq z \leq 4$ . We take into account the absorption of Lyman-limit photons by HI and dust in the interstellar medium (ISM) of the galaxies. We find that the background Lyman-limit flux due to galaxies might dominate (or be comparable to) the contribution from quasars at almost all redshifts if the absorption by HI in the ISM is neglected. The ISM HI absorption results in a severe diminishing of this flux—by almost three orders of magnitude at high redshifts to between one and two orders at  $z \simeq 0$ . Though the resulting galaxy flux is completely negligible at high redshifts, it is comparable to the quasar flux at  $z \simeq 0$ .

**Key words:** cosmology—galaxy evolution—background flux—DLA absorbers

## 1 INTRODUCTION

The study of the evolution of the ionization state of the diffuse intergalactic medium (IGM) is crucial to understanding the formation of structures in the universe. An important input in this study is the intensity and evolution of the background hydrogen-ionizing flux. The universe is observed to be highly ionized at high redshifts (Gunn & Peterson 1965, Giallongo *et al.* 1994) and it is widely believed that the main mechanism of ionization is photoionization by photons at and below the Lyman-limit. This view is borne out by estimates of background hydrogen-ionizing flux as inferred by the ‘proximity effect’ which fixes the value of this flux,  $J_{\text{ion}} \simeq 10^{-21 \pm 0.5} \text{ erg s}^{-1} \text{ cm}^{-2} \text{ Hz}^{-1} \text{ sr}^{-1}$  (Bajtlik, Duncan & Ostriker 1988; Bechtold 1994; Giallongo *et al.* 1996; Cooke *et al.* 1997) for  $2 \lesssim z \lesssim 4.5$ . It is not clear whether the observed quasars can provide sufficient contribution to the flux implied by this effect at  $z \geq 3$  (Miralda-Escudé & Ostriker 1990; Giroux & Shapiro 1996; Haardt & Madau 1996; Cooke *et al.* 1997). In light of this fact, it was speculated that high-redshift star-forming galaxies could be the dominant contributor to this background flux (Songaila, Cowie & Lilly 1990). At smaller redshifts, there is a greater uncer-

tainty in the level of this flux (Kulkarni & Fall 1993; Maloney 1993; Vogel *et al.* 1995; Reynolds *et al.* 1995); however, a tight upper limit of  $J_{\text{ion}} < 8 \times 10^{-23} \text{ erg s}^{-1} \text{ cm}^{-2} \text{ Hz}^{-1} \text{ sr}^{-1}$  at  $z \simeq 0$  exists from H $\alpha$  observations (Vogel *et al.* 1995). If this flux is entirely due to the background hydrogen-ionizing photons then the contribution of quasars falls short of the observed value by nearly an order of magnitude at  $z \simeq 0$  (Madau 1992; Haardt & Madau 1996).

Recent years have seen tremendous progress in understanding the formation and evolution of galaxies at moderate and high redshifts. Prominent observations which made it possible are the probing of the evolution of galaxies with  $z \leq 1$  by the Canada-France Redshift Survey (CFRS) (Lilly *et al.* 1995), the discovery of high-redshift galaxies using the UV drop-out technique (Steidel *et al.* 1996) in the Hubble Deep Field (HDF) (Madau *et al.* 1996; Sawicki *et al.* 1997; Connolly *et al.* 1997), and a better understanding of the evolution of the neutral hydrogen content and average metallicity of DLA systems from  $z \simeq 0$  to  $z \simeq 4$  (Lanzetta *et al.* 1995, Pettini *et al.* 1997). Several theoretical attempts have been made to explain these observations (Madau 1996, 1997; Fall *et al.* 1996; Frenk *et al.* 1996; Guiderdoni *et al.* 1997b, hereafter GHBM). These observations give valuable

clues about the history of star formation and the comoving emissivity in several wavebands in the universe upto  $z \simeq 4$  and have provided a unique opportunity to model and study the contribution of star-forming galaxies to the background hydrogen-ionizing flux (for recent attempts to estimate the hydrogen-ionizing flux from star-forming galaxies for  $z \leq 1.5$  see Giallongo *et al.* (1997); Deharveng *et al.* (1997)).

The CFRS observations give the evolution of cosmic emissivity at  $\lambda \simeq 2800 \text{ \AA}$  (in the rest frame of the emitter) for  $z \leq 1$  while the HDF observations estimate the emissivity at  $\lambda \simeq 1620 \text{ \AA}$  for  $2.5 \leq z \leq 4$ . Our aim in this paper is to extrapolate the results from these important UV wavelengths to calculate the emissivity (and background flux) at the Lyman-limit wavelength. The hydrogen-ionizing photons are emitted by massive stars with lifetimes  $\simeq 10^7$  years, so their flux is not sensitive to the history of galaxy evolution, which has much larger time scales. Conversely, one can view it as a direct measurement of the instantaneous SFR. The conversion of emissivity from the wavelengths probed by HDF and CFRS to  $912 \text{ \AA}$  requires knowledge of three factors:

- the absorption of photons with  $\lambda \leq 912 \text{ \AA}$  within the stellar atmosphere.
- the amount of dust and the spectral index of dust absorption coefficient in the interstellar medium.
- the amount of neutral hydrogen in the interstellar medium.

The first factor is fixed by stellar atmosphere models and depends mainly on the choice of IMF which is guided by our ability to reproduce observed colours of galaxies.

In extrapolating the amount of dust absorption from the observed value at  $1620 \text{ \AA}$  (or  $2800 \text{ \AA}$ ) to the Lyman-limit wavelength, it is important to know the amount of dust in the galaxies as accurately as possible, because  $A_{912}/A_V \simeq 5$  as compared to  $A_{1600}/A_V \simeq 2.5$ . Therefore a small uncertainty in the dust extinction at UV wavelengths translates into a much larger error in the extinction at the Lyman-limit. We can use FIR data available to fix the amount of dust at  $z \simeq 0$ . At higher redshift, we can fix it by matching the observed average metallicity of DLA absorbers (Pettini *et al.* 1997) and by reproducing the cosmic infrared background (CIB) reported by Puget *et al.* (1996).

The most crucial factor in determining the absorption of hydrogen-ionizing photons in the ISM is the amount of HI and its distribution in galaxies. We can model this by using the available data on DLA absorbers which give the evolution of the average HI content of these clouds for  $0 \leq z \leq 4$  (Lanzetta *et al.* 1995). In our study we have to assume that DLA absorbers belong to the same population of galaxies as the ones that are observed in emission in the CFRS and HDF. No clear consensus has been reached on this point yet, but recent observations may support the explanation that the DLA absorbers are either thick rotating disks or protogalactic clumps (Haenelt *et al.* 1997; Prochaska & Wolfe 1997). Thereafter We assume the HI, dust, and stars to be homogeneously distributed in the ISM. This assumption gives the maximum possible HI absorption and allows us to obtain a lower limit on the fraction of Lyman-limit photons escaping from galaxies. We shall also briefly discuss the implications of the clumpiness of HI.

We use a semi-analytic model of galaxy formation to

study the evolution of background hydrogen-ionizing flux for  $0 \leq z \lesssim 4$  (for details see, e.g. GHMB). In §2, we describe the relevant features this model and its various assumptions. The basic method of obtaining the background ionizing flux given the comoving emissivity and various sources of intergalactic absorption is also briefly described in this section. Our results are detailed in §3. In §4 we discuss various uncertainties and possible improvements in our estimates and summarize our conclusions in §5.

## 2 SEMI-ANALYTIC MODELS AND HYDROGEN-IONIZING FLUX

We do not attempt to give a detailed description of semi-analytic models of galaxy formation and evolution. Readers interested in details are referred to the recent paper GHBM and references therein. We just introduce and define the parameters required for our work.

### 2.1 Collapse of halos and cooling

We consider fluctuations in the matter density distribution at high redshift to be spherically symmetric (“Top Hat” approximation, see eg. Peebles 1980) on galactic scales. As a result of the violent relaxation process that they undergo after collapsing at redshift  $z_{coll}$ , such halos virialize. One can then use the peaks formalism (Bardeen *et al.* 1986) to compute the mass distribution of such halos, as in Lacey and Silk (1991) and Lacey *et al.* (1993), for a given cosmological model.

The baryonic gas subsequently radiates away its energy, falling deeper and deeper in the potential well, until it reaches rotational equilibrium and settles into a disk-like structure. Thus, the length scale  $r_{disk}$ , of the cold gas exponential disk can be inferred from the initial radius  $r_v$  by conservation of angular momentum  $r_{disk} \simeq \lambda_J r_v$  where  $\lambda_J$  is the dimensionless spin parameter (Fall & Efstathiou 1980). Only disks can form in this formalism. The formation of elliptical galaxies (and of bulges of spiral galaxies) has to be explained by the merging of disks. Kauffmann *et al.* (1993) and Cole *et al.* (1994) showed that this process can explain the current fraction of giant ellipticals among bright galaxies.

### 2.2 Star formation

It is well known that local physical processes governing star formation are complex and depend on various parameters. Nevertheless, it seems that, on galaxy scales, one can phenomenologically define a mean Star Formation Rate (hereafter SFR) per unit surface density, which is proportional to the total gas surface density (neutral plus molecular) divided by the dynamical time scale of the disk (Kennicutt 1989, 1997). Hence we assume that the star formation time scale  $t_\star$  is proportional to the dynamical time scale of the disk:  $t_\star \equiv \beta(z) t_{dyn}$  where  $t_{dyn} \equiv 2\pi r_{disk}/V_c$ . In the previous formula  $V_c = (GM/r_v)^{1/2}$  is the circular velocity of the dark matter halo of mass  $M$ , and  $\beta(z)$  is our first free parameter, that we allow to vary with redshift in order to reproduce

the shape of the cosmic comoving emissivity at 1620 Å and 2800 Å from  $z = 0$  to  $z = 4$ . The SFR at time  $t$  is then computed as follows:

$$SFR(t) = \frac{M_{\text{gas}}(t)}{t_*}. \quad (1)$$

As shown in GHBM (their fig. 3), using such a prescription allows one to match the average value and width of the observed distribution of “Roberts time” for a  $z \simeq 0$  bright disk galaxies sample given by Kennicutt *et al.* (1994), just by taking  $\beta(0) \simeq 100$ . Furthermore, as pointed out by these authors, the shape of the cosmic comoving star formation rate density curve (their fig. 9) suggests a strong evolution of  $\beta$  with redshift. Our model shares the same spirit: we consider the star formation history in the universe as a sum of contributions from a population of quiescent star-forming galaxies and a population of starburst galaxies whose respective proportions are modelled through  $\beta(z)$ . We allow  $\beta(z)$  to vary from  $\simeq 0.5$  to  $\simeq 200$  which respectively corresponds to starburst and quiescent mode of star formation.

### 2.3 Stellar feedback

Stellar feedback is modelled following the original work by Dekel and Silk (1986). It stems from massive star explosions which expel gas from the galaxies, preventing further star formation to occur. Physically, when the thermal energy ejected by supernovae becomes greater than the binding energy of the halo, one expects such winds to be triggered with a certain efficiency. One can then compute the mass fraction of stars forming before the galactic wind:

$$F_* \equiv \frac{M_*}{(M_* + M_{\text{gas}})} = (1 + (V_{\text{hot}}/V_c)^\alpha)^{-1}, \quad (2)$$

where  $V_{\text{hot}}$  and  $\alpha$  are obtained through a fit based on SPH simulations of galaxy formation in which most of the feedback effect is due to momentum exchange as in Cole *et al.* (1994). But one should bear in mind that there is much uncertainty on these parameters mostly due to the treatment of supernova remnant interactions with the interstellar medium. Moreover, as pointed out by Efstathiou (1992) and Blanchard *et al.* (1992), there is likely to be an overall high- $z$  re-heating of the intergalactic medium which could prevent cooling in halos with circular velocities below  $V_c \sim 20$  to 50 km s $^{-1}$ , and possibly as high as  $\sim (200)^{1/3} V_c$  in case of adiabatic collapse. To sum up, the situation is very complicated because we lack a global theory of feedback processes. Therefore, we adopt a rather crude but simple approach to the problem: we do not attempt to model the redshift dependence of local or global feedback in this paper, but we just consider the values derived from numerical simulations for a typical ten percent feedback efficiency of momentum exchange. They give  $\alpha = 5$  and  $V_{\text{hot}} = 130$  km s $^{-1}$ . In the following, we keep the same value for  $\alpha$  and allow our second free parameter  $V_{\text{hot}}$  to vary between 100 and 130 km s $^{-1}$ .

### 2.4 Stellar populations

We use a coupled model of spectrophotometric and chemical evolution in order to compute the age dependence and metallicity of the gas content, and of the UV to NIR spectra of the stellar populations in a self-consistent way. The

end-product of these models are time dependent synthetic spectra and gas/metallicity evolution of galaxies. The model which is used here is based upon a new numerical scheme (isochrone), as well as on up-graded Geneva stellar tracks and yields, and will be described in Devriendt, Guiderdoni and Sadat (1998, in preparation). The photometric properties of galaxies which are our main interest in this study are obtained after taking into account the intrinsic extinction due to both the neutral hydrogen absorption below 912 Å and the dust (see following section).

### 2.5 Dust and gas absorption

Some of the energy released by stars in the UV and optical is absorbed by dust and HI gas (for wavelengths shorter than 912 Å) and re-emitted in the IR and submm ranges. We would like to emphasize the difficulty of estimating these absorption processes since one has to address the complicated and crucial issue of the geometrical distribution of dust and gas relatively to stars. In the following, we assume that the gas is distributed in an exponential disk with mean HI column density at time  $t$ ,

$$\langle N_{\text{HI,ISM}}(t) \rangle = M_{\text{gas}}(t) / 1.4 m_{\text{H}} \pi r_g^2, \quad (3)$$

where  $r_g \equiv f_c r_{\text{disk}}$  is the truncation radius of the gaseous disk,  $f_c$  being our third free parameter. The factor 1.4 accounts for the presence of helium. The mean optical thickness inside  $r_g$  is given by:

$$\begin{aligned} \langle \tau_\lambda(t) \rangle &= \left( \frac{A_\lambda}{A_V} \right)_{Z_\odot} \left( \frac{Z_g(t)}{Z_\odot} \right)^s \left( \frac{\langle N_{\text{HI,ISM}}(t) \rangle}{2.1 \cdot 10^{21} \text{ at cm}^{-2}} \right) \\ &+ \langle N_{\text{HI,ISM}}(t) \rangle \sigma_{\text{HI}} \left( \frac{\lambda}{912 \text{ Å}} \right)^3 \Theta(912 \text{ Å}), \end{aligned} \quad (4)$$

where the first term contains:

- the extinction curve for solar metallicity as measured by Mathis *et al.* (1983).
- the gas metallicity ( $Z_g(t)$ ) dependence of the extinction curve which is modelled as in Guiderdoni and Rocca-Volmerange (1987) and Franceschini *et al.* (1991, 1994), according to power-law interpolations based on the Solar Neighbourhood and the Magellanic Clouds, with  $s = 1.35$  for  $\lambda < 2000$  Å and  $s = 1.6$  for  $\lambda > 2000$  Å.

The second term is due to the hydrogen absorption and hence is only used for wavelengths shorter than 912 Å ( $\Theta$  being the Heavyside function),  $\sigma_{\text{HI}} = 6.3 \times 10^{-18} \text{ cm}^2$  is the hydrogen ionization cross section at the threshold.

Light scattering by dust grains is also modelled and the final optical depth is averaged over inclination angle assuming stars, dust and gas are homogeneously mixed as in Dwek and Városi (1996). These authors extended the radiative transfer calculation in a spherically symmetric ISM to the case of an ellipsoid which is more relevant for our study. The results are quite similar to those obtained with a classic “slab” geometry where stars, dust and gas are distributed with the same scale height, and seem to satisfy the estimates of extinction given by Andreani and Franceschini (1996). As the galaxy is optically thick to Lyman-limit photons, this homogeneous distribution of stars and dust implies

that only a tiny fraction ( $\simeq 1/\langle\tau_{912}\rangle$ ) of Lyman-limit photons will be able to escape from the galaxy: the ones emitted by stars located in a thin outer shell (with column density  $\simeq 1/\sigma_{\text{HI}} \simeq 1.6 \times 10^{17}$  at  $\text{cm}^{-2}$ ) of the gaseous disk. This procedure enables one to compute the bolometric luminosity absorbed by dust and re-processed in the IR/submm.

## 2.6 Dust emission

Here, we will not give details on how we derive the IR/submm spectrum (see GHB), but just briefly outline the steps that lead to the emission spectrum. As mentioned in the previous section, we compute the optical depth of the disks, and the amount of bolometric luminosity absorbed by dust. The last step consists in the computation of emission spectra of galaxies in the IR/submm wavelength bands. This is completed by using a three-component dust model (Polycyclic Aromatic Hydrocarbons, Very Small Grains and Big Grains), which is described in Désert *et al.* (1990). The method employed is very similar to that developed by Maffei (1994), and is based upon observational correlations of the IRAS flux ratios with the total IR luminosity (Devriendt, Guiderdoni & Sadat 1998, in preparation).

## 2.7 Hydrogen-Ionizing Flux

Once one has computed the fraction of hydrogen ionizing photons that effectively escape from the galaxies, one still has to estimate the optical depth of the inter-galactic medium. This section describes the prescription we use. Given the comoving emissivity of hydrogen-ionizing flux  $\epsilon(\nu, z)$ , the specific intensity of the background flux  $J(\nu_0, z_0)$  (in  $\text{erg s}^{-1} \text{cm}^{-2} \text{Hz}^{-1} \text{sr}^{-1}$ ) is calculated using (Bechtold *et al.* 1987):

$$\begin{aligned} J(\nu_0, z_0) &= \frac{cH_0^{-1}}{4\pi} \int_{z_0}^{\infty} dz \frac{(1+z_0)^3}{(1+z)^5(1+\Omega_0 z)^{1/2}} \\ &\times \epsilon(\nu, z)(1+z)^3 \exp[-\tau(\nu_0, z_0, z)] \end{aligned} \quad (5)$$

Here  $\tau(\nu_0, z_0, z)$  is the optical depth for a photon emitted at redshift  $z$  with frequency  $\nu$  and observed at redshift  $z_0$  with frequency  $\nu_0 = \nu(1+z_0)/(1+z)$ . In this paper we assume that this optical depth is due to HI in Lyman- $\alpha$  system clouds encountered along any line of sight. The absorption due to singly ionized helium is negligible in determining the hydrogen ionizing flux. Neutral helium is always a sub-dominant species in the Lyman- $\alpha$  clouds in case the background flux is dominated by quasars or star-forming galaxies. Therefore we neglect the absorption due to neutral helium. We also neglect the absorption due to diffuse HI in the intergalactic medium, because there is no evidence of its presence.

The line-of-sight average optical depth  $\tau_{\text{Ly}}(\nu_0, z_0, z)$  due to Poisson-distributed Lyman- $\alpha$  clouds can be expressed as (Paresce *et al.* 1980):

$$\begin{aligned} \tau_{\text{Ly}}(\nu_0, z_0, z) &= \int_{z_0}^z \int_0^{\infty} dz dN_{\text{HI,IGM}} \mathcal{P}(N_{\text{HI,IGM}}, z) \\ &\times \{1 - \exp[-N_{\text{HI,IGM}} \sigma_{\text{HI}}(\nu)]\}. \end{aligned} \quad (6)$$

Here  $N_{\text{HI,IGM}}$  is the neutral hydrogen column density of

the Lyman- $\alpha$  clouds.  $\mathcal{P}(N_{\text{HI,IGM}}, z)$  is the average number of clouds with HI column density between  $N_{\text{HI,IGM}}$  and  $N_{\text{HI,IGM}} + dN_{\text{HI,IGM}}$  in a redshift range  $z$  to  $z + dz$  along any line of sight. With the existing observations, it is not possible to uniquely fix the form of  $\mathcal{P}(N_{\text{HI,IGM}}, z)$  from  $0 \lesssim z \lesssim 4$ . For  $z \geq 1.7$  we take model 3 of Giroux & Shapiro (1996) for Lyman- $\alpha$  clouds, with  $N_{\text{HI}} \leq 1.5 \times 10^{17} \text{ cm}^{-2}$ . For  $z \leq 1.7$ , we take the redshift evolution given by Bahcall *et al.* (1993) and normalize the number of clouds per unit redshift at  $z = 1.7$  with model 3 of Giroux and Shapiro 1996. This is consistent with the findings of Bahcall *et al.* (1993) for clouds with equivalent width,  $W \geq 0.32 \text{ \AA}$  ( $N_{\text{HI}} = 1.5 \times 10^{14} \text{ cm}^{-2}$ ). For Lyman-limit systems ( $N_{\text{HI}} \geq 1.5 \times 10^{17} \text{ cm}^{-2}$ ), the results of Stengler-Larrea *et al.* (1995) are taken for  $0 \leq z \leq 4$ . The emissivity  $\epsilon(\nu, z)$  is determined from the galaxy evolution models which fulfill a certain criterion described in the next section. The contribution of ionizing flux from 'reprocessing' inside Lyman- $\alpha$  clouds is neglected in our estimates (for details see Haardt & Madau 1996).

## 3 RESULTS

### 3.1 Parameters

In the following, we consider the so-called Standard Cold Dark Matter (SCDM) model with  $H_0 = 50 \text{ km s}^{-1} \text{ Mpc}^{-1}$ ,  $\Omega_0 = 1$ ,  $\Lambda = 0$ , and  $\sigma_8 = 0.67$ . We take the baryonic fraction to be  $\Omega_B = 0.05$ , consistent with primordial nucleosynthesis. Our approach in this paper is to work within the framework of one cosmological model and a single set of values of the parameters, and to assume that all the changes that may occur from altering these choices can be compensated by appropriately adjusting the free parameters of the semi-analytic models of galaxy formation. As a matter of fact, it seems that the uncertainties from various galactic evolution processes like interactions, mergers, etc. are more important than the potential influence of the background cosmology and structure formation models (Heyl *et al.* 1995).

For simplicity, we take a Salpeter Initial Mass Function (hereafter IMF) with index  $x = 1.35$ . Stars have masses  $0.1 \leq m \leq 120 M_{\odot}$ , and we assume that the mass fraction forming dark objects with masses below  $0.1 M_{\odot}$  is negligible. Though we have used a Salpeter IMF throughout this paper, it is possible that the IMF at high redshift is top-heavy and hence produces more UV flux. We ran a few models with a top-heavy IMF at high- $z$  and noticed that we overestimate the metal production by a considerable amount. However, these models may be allowed if a large fraction of metals are blown away with galactic winds in the IGM. Present observations suggest that as much as half the metals at high redshifts are in small column density Lyman- $\alpha$  clouds (Songaila & Cowie 1996), so it may not be unrealistic to assume that a substantial fraction of metals are blown from the galaxies. However, it can enhance the Lyman-limit flux by a factor of a few units at high redshifts which does not affect our results significantly (see the discussion the section 3.3).

In order to put robust bounds on the hydrogen-ionizing emissivity  $\epsilon(\nu, z)$  coming from galaxies, we define two models which are representative of the uncertainties in the high- $z$  measurement of the 1620  $\text{\AA}$  cosmic emissivity (Madau *et al.* 1996, Sawicki *et al.* 1997). Model I gives a fairly good fit

of Madau *et al.*'s results at high redshift. Model II matches values determined by Sawicki *et al.* (1997). Both models are completely defined by the three parameters previously mentioned. The first free parameter (the SFR efficiency parameter),  $\beta(z)$  is shown in Fig. 1 for both models. Its strong evolution with redshift is necessary to reproduce the sharp decrease of the cosmic comoving emissivity observed by the CFRS but the results are not very sensitive to the shape of the function used provided the peak is located at the right position  $z \simeq 1.5$  and that  $0.5 \leq \beta(z) \leq 200$ . For instance, Fig. 1 clearly shows that even though  $\beta(z)$  evolves more strongly in model II (dashed curve) than in model I, there is no drastic difference in the cosmic emissivity around the peak in both models.

The value of the concentration parameter  $f_c$  is quite poorly known but, as pointed out in GHBM (their figure 6), the prescription given above allows one to match quite well the measured FIR and mm emission of a flux-limited sample dominated by mild starbursts and luminous IR galaxies (Franceschini and Andreani 1995) provided one takes  $f_c \simeq 2.7$ . However, such observations tend to pick out galaxies with central, dense regions undergoing star formation (Sanders & Mirabel 1996) and therefore are biased to give smaller values of  $f_c$ . On the other hand, as argued by Mo *et al.* (1997) and Lobo and Guiderdoni (1998) (in preparation), semi-analytic models predict too small disk radii in the SCDM as compared to observations. Hence, we fix the value of  $f_c$  to get the correct distribution of DLA (Fig. 2) which is based on the absorption properties of these clouds.  $f_c$ 's influence concerns mainly the HI distribution : the larger the value of this parameter, the more extended the HI exponential disks and the fewer the DLA systems. There is likely to be a redshift dependence of this parameter, simply due to the fact that mergers have a well-known tendency to concentrate the gaseous content of disks. However, we did not try to model that effect but rather took an average value of the parameter over redshift. Averaged values  $f_c = 7$  for model I and  $f_c = 5$  for model II, allow us, as shown in Fig. 2, to reproduce quite well the column density distribution of DLA at several redshifts.

Finally, as discussed in the last section, the value of the third parameter (the feedback parameter),  $V_{hot}$ , is difficult to determine. However, it has very little influence on the results because it mainly affects the faint-end slope of the HI mass function, so we just tuned it in order to get the right amount of HI in DLA systems at high- $z$  (Storrie-Lombardi *et al.* 1996). Such a requirement yields values for Model I and II of 120 and 100  $\text{km s}^{-1}$  respectively.

### 3.2 Luminosity Densities

Figs. 3 and 4 show results for the two models discussed above. The "merit" of a model is judged by its ability to predict correctly the evolution of emissivities in various wavebands, the evolution of  $\Omega_{\text{HI}}$  and the average metallicity of DLA absorbers from  $0 \simeq z \leq 4$ . The predicted evolution of the Lyman-limit emissivities—with or without absorption by HI in the interstellar medium of galaxies—is also shown in the figures. As seen in Figs. 3 and 4, the two models capture fairly well the broad features of the universe upto  $z \simeq 4$ . The only discrepancy between the observations and theoretical estimates is that these models predict too

high a value of  $\Omega_{\text{HI}}$  at  $z \simeq 0$  (Figs. 3a and 4a). To investigate this point in detail, we show in Fig. 2 the HI mass function at  $z = 0$  (Zwaan *et al.* 1997), along with the distribution of HI column density in DLA absorbers at three redshifts (Lanzetta *et al.* 1995). Although the agreement at higher redshift is seen to be quite good, the disagreement at  $z = 0$  can be noticed in Fig. 2d. Whereas the deviation of theoretical predictions from the observed HI mass function at small HI masses is probably due to our feedback prescription, we also overestimate slightly the HI content for  $10^9 \text{ M}_\odot \leq M_{\text{HI}} \leq 5 \times 10^{10} \text{ M}_\odot$ . The disagreement at large HI masses is more important because much of the hydrogen-ionizing photons are seen to be emitted by the largest masses in our models. Nevertheless, this discrepancy, which would result in an overestimate of the HI absorption in the ISM in evaluating the hydrogen-ionizing emissivity, is somewhat alleviated by the fact that the star formation rate is also higher because of its proportionality to the gas mass (Eq.(1)).

The emissivity of Lyman-limit photons depends sensitively on dust and HI absorption in the ISM. At  $z \simeq 0$ , the amount of dust in galaxies is fixed by matching the energy re-radiated in the FIR and mm bands with IRAS results at  $60 \mu\text{m}$ , as shown in Figs. 3 and 4. At high redshifts, there is a greater uncertainty in the average amount of dust in galaxies. We use Eq. (4), which relates the dust optical depth with the average hydrogen column density  $\langle N_{\text{HI,ISM}}(t) \rangle$  and metallicity  $Z_g(t)$  of a galaxy, to fix the dust content in a galaxy to within the observational uncertainties in the evolution of  $\langle N_{\text{HI,ISM}}(t) \rangle$  and  $Z_g(t)$ . The recent detection of the CIB (Puget *et al.* 1996; Guiderdoni *et al.* 1997a) can also be used to constrain the history of dust emission in the universe. GHBM used semi-analytic models of galaxy formation to explain the observed CIB. We plot results of their models (A) and (E), which successfully explain Puget *et al.*'s results, in Figs. (3b) and (4b) along with the prediction of our models at  $\lambda = 60 \mu\text{m}$ . It is quite clear that there is a good agreement between the two results. Therefore, we believe that our method allows us to get a fair estimate of dust absorption for  $0 \leq z \leq 4$ .

As is evident from Figs. 3 and 4, the HI absorption in the ISM is the most important factor in determining the hydrogen-ionizing emissivity. It is customary to compute the emissivity of galaxies and multiply by a constant escape fraction to account for this uncertainty (see e.g, Giallongo *et al.* 1997). We model this by using Eq. (4) for the optical depth of the neutral hydrogen in a galaxy. As discussed above, in a geometry where the gas and stars are homogeneously mixed, it just means that a factor  $1/\langle \tau_{912} \rangle$  of all the hydrogen-ionizing photons can escape the galaxy. As  $\langle \tau_{912} \rangle \gg 1$ , the validity of such an assumption depends crucially on the relative distribution of stars and neutral hydrogen in the ISM. However, it should be pointed out that a homogeneous distribution gives an overestimate of the absorption, i.e. an optically thick but clumpy medium will always result in less absorption, and therefore the average emissivity we estimate is a secure lower limit on the hydrogen-ionizing emissivity from star-forming galaxies.

### 3.3 Galactic Background Lyman-limit Flux

The evolution of the background flux of Lyman-limit photons for various cases discussed above is shown in Fig. 5

along with the available observations at low and high redshifts. The high redshift data shown in Fig. 5 is taken from Cooke *et al.* (1997). Other high redshift proximity effect calculations such as the one by Giallongo *et al.* (1996) give  $J_{\text{ion}} \simeq (5 \pm 1) \times 10^{-22} \text{ erg s}^{-1} \text{ cm}^{-2} \text{ Hz}^{-1} \text{ sr}^{-1}$  independent of the redshift for  $2 \leq z \leq 4$ . The evolution of the quasar contribution is also shown, based on the quasar luminosity function derived by Pei (1995). All the observational results discussed before give the background hydrogen-ionizing flux,  $J_{\text{ion}}$ , as opposed to the Lyman-limit flux we calculate. They are related as:  $J_{\text{ion}} = 3/(3 + \delta) \times J_{912}$ , where  $\delta$  is the spectral index of the UV background flux (Miralda-Escudé & Ostriker 1992). For quasar and galaxy UV backgrounds,  $\delta \simeq 1-2$  (see for instance Miralda-Escudé & Ostriker 1990). We scale all the values of  $J_{\text{ion}}$  assuming  $\delta = 1$ , at all redshifts, in Fig. 5. We also show the flux without dust absorption to gauge the relative importance of dust absorption as compared to HI absorption. It should be pointed out that the curves without dust absorption are not normalized to HDF and CFRS fluxes at other wavebands so they cannot be taken as realistic estimates of Lyman-limit flux; their only purpose is to estimate the relative importance of dust and HI extinction of the Lyman-limit flux. As is clearly seen, dust absorption decreases the HI flux typically by a factor of a few while the HI absorption can diminish it by nearly three orders of magnitude at high redshift.

If the absorption of Lyman-limit photons by HI in the ISM of a galaxy is neglected, then the background hydrogen-ionizing flux from star-forming galaxies can be comparable to or dominate the flux from quasars and might make up for the extra flux which might be required to explain the proximity effect (Cooke *et al.* 1997). However, we believe that it is highly unrealistic to completely neglect the HI absorption in the ISM. As Fig. 5 shows, the ionizing flux at  $z \simeq 3$  decreases by more than three orders of magnitude when this absorption is taken into account. Such a decrease cannot be compensated by the uncertainties in our analysis and therefore it seems unlikely that star-forming galaxies dominate the hydrogen-ionizing flux at high redshifts. The situation is quite different at smaller redshifts. At  $z \simeq 0$ , even the lower limit to galactic flux, (see the lower set of curves in Fig. 5) might be more than the quasar contribution. As discussed above, we overestimate the HI absorption in the ISM and so the value of the ionizing flux at  $z \simeq 0$  could be higher by a factor of a few over the values shown in Fig. 5. Therefore, though the quasars are likely to dominate the background hydrogen-ionizing flux at high- $z$ , the substantial contribution to this flux at smaller redshift is very likely to be due to star-forming galaxies. Our results are in qualitative agreement with the recent estimates of Giallongo *et al.* (1997) and Deharveng *et al.* (1997).

The nature of the ionizing background at high redshifts is also indicated by the recent observation of He II at high redshifts (see e.g., Davidsen *et al.* 1996). These observations allow one to estimate of the softness parameter,  $S_L \equiv J_{912}/J_{228}$ . At  $z \simeq 3$ ,  $S_L \simeq 40$  for quasar-dominated background flux (Haardt & Madau 1996) but can be as high as 1000 for background flux dominated by star-forming galaxies (Miralda-Escudé & Ostriker 1990). However, various uncertainties in the modelling of Lyman- $\alpha$  clouds at high- $z$  as well as in the observations do not allow a firm conclusion on the softness of the ionizing background at

high- $z$  (Sethi & Nath 1997). We also note that the recent numerical simulations of Lyman- $\alpha$  absorbers show a good match with the observations if a low value of  $J_{912}$  ( $\simeq 1-4 \times 10^{-22} \text{ erg s}^{-1} \text{ cm}^{-2} \text{ Hz}^{-1} \text{ sr}^{-1}$ ) and a quasar-like spectrum is adopted (Miralda-Escudé *et al.* 1996, Zhang *et al.* 1996). Therefore, it seems that apart from a few estimates of the proximity effect (Cooke *et al.* 1997), the value of ionizing flux implied by the observed quasars may suffice to explain other observations at high- $z$ , which is in agreement with our conclusions.

## 4 DISCUSSION

What are the various sources of uncertainties and errors in our estimates? We have assumed that the stars, dust, and HI are homogeneously distributed in the galaxy, which, as already discussed, is not entirely justified. In this section, we discuss the possible implications of relaxing this assumption.

Throughout this paper we use Eq. (1) and (4) which give the SFR and optical depth averaged over the entire disk. We experimented with a few cases in which we considered the effect of *local* SFR and  $\tau_\lambda$ . We subdivided the disk in shells of increasing radii and estimated the SFR and optical depth averaged over these shells; this enabled us to calculate the amount of Lyman-limit photons escaping from the disk as a function of the radial distance. In this case, both the SFR and the optical depth decrease towards the outer regions of the galaxy. The aim of this exercise was to investigate whether the decrease in SFR is less important than the decrease in the optical depth, and a relatively larger fraction of Lyman-limit photons could escape from outer parts of a galaxy. However, this does not happen because, for our values of  $f_c$ , the disk remains optically thick to Lyman-limit photons even at the truncation radius  $r_g$  where the HI column density  $N_{\text{HI,ISM}}(r_g) = \langle N_{\text{HI,ISM}} \rangle / 1.6 \times f_c^2 \exp(-1.6 \times f_c)$ , which means that even there the fraction of Lyman-limit photons which can escape remains  $\simeq 1/\tau_{912}$ . As both the SFR and  $\tau_{912}$  are proportional to  $\langle N_{\text{HI,ISM}} \rangle$  (Eqs. (3) and (4)), the decrease in the optical depth is compensated by a similar decrease in SFR. Therefore, the total emergent flux from a galaxy remains the same whether we consider quantities averaged over the entire disk or we sum the contributions of all the shells.

Though it is extremely difficult to accurately model the clumpiness of the ISM, we give below qualitative argument to gauge its effect on the HI ISM absorption. Let us assume that all the HI in the ISM is in the form of HI clouds with number of clouds per column density  $f(N_{\text{HI,ISM}})$  distributed as:

$$f(N_{\text{HI,ISM}}) \equiv \frac{dN}{dN_{\text{HI,ISM}}} = AN_{\text{HI,ISM}}^{-\gamma} \quad (7)$$

The optically thin clouds ( $N_{\text{HI,ISM}} \leq \sigma_{\text{HI}}^{-1}$ ) mimic the homogeneous part of the ISM while the clouds with  $N_{\text{HI,ISM}} \geq \sigma_{\text{HI}}^{-1}$  correspond to the clumpy ISM. The total average optical depth, along any line of sight, due to Poisson-distributed clouds with this distribution is:

$$\begin{aligned} \langle \tau_{\text{ISM}}^C \rangle &\equiv \int_{N_{\text{HI,ISM}}(\text{min})}^{N_{\text{HI,ISM}}(\text{max})} [1 - \exp(-N_{\text{HI,ISM}}\sigma_{\text{HI}})] \\ &\times f(N_{\text{HI,ISM}}) dN_{\text{HI,ISM}}. \end{aligned} \quad (8)$$

Our aim is to calculate the absorption from the clumpy part of the ISM and see what difference it would make if the same amount of matter was distributed homogeneously. To do that, we are interested in the ratio of the average optical depth of the clumpy medium from Eq. (8) and  $\langle \tau_{ISM}^H \rangle \equiv \langle N_{HI,ISM} \rangle \sigma_{HI}$ , the optical depth if the HI in the clumpy medium was distributed homogeneously. We further assume that the ionizing stars are located outside the clouds in order for the HI absorption to be minimum. For the distribution given by Eq. (7), we get:

$$\frac{\langle \tau_{ISM}^C \rangle}{\langle \tau_{ISM}^H \rangle} = \frac{(-\gamma + 2)}{(-\gamma + 1)} \frac{\left[ N_{HI,ISM}^{(\gamma+1)}(\max) - N_{HI,ISM}^{(\gamma+1)}(\min) \right]}{\left[ N_{HI,ISM}^{(\gamma+2)}(\max) - N_{HI,ISM}^{(\gamma+2)}(\min) \right]} \frac{1}{\sigma_{HI}} \quad (9)$$

Observations of HI clouds in the ISM of our galaxy suggest the clouds have a distribution given by Eq. (7) with  $1.6 \leq \gamma \leq 2.2$  for  $10^{18} \text{ cm}^{-2} \leq N_{HI,ISM} \leq 10^{22} \text{ cm}^{-2}$  (Dickey & Garwood, 1990), which corresponds to the clumpy part of the ISM. For these values,  $0.01 \leq \langle \tau_{ISM}^C \rangle / \langle \tau_{ISM}^H \rangle \leq 0.03$  ( $\gamma = 2$  is excluded as Eq. (9) is not valid for this value). Our simple analysis suggests that the average optical depth from the clumpy part of the ISM is negligible as compared to the homogeneous part; and much of the absorption is caused by the fraction of HI in the homogeneous medium (or optically thin clouds) in the ISM. There is a great amount of uncertainty in determining the fraction of the homogeneously distributed HI in the ISM. If, for the purpose of this paper, we roughly assume that the HI is distributed equally between the homogeneous and the clumpy ISM, as might be the case for our galaxy, then our analysis suggests that the average optical depth of the ISM is halved as compared to the case when the entire ISM is made up of homogeneously distributed HI.

It is known that a significant fraction of young stars form inside optically thick clouds which suggests that the arguments given above underestimate the absorption. On the other hand, most of the ionizing stars form in OB associations. The UV photons from these stars could puncture the layer of neutral hydrogen to escape into the galactic halo. This fact can be used to explain the existence of HII at large scales heights (Reynolds 1984) which requires a large fraction of the photons to escape in the halo (Dove & Shull 1994). However, it is not clear what fraction of this ionizing flux can escape the halo of a galaxy. The observational status of hydrogen ionizing flux from other galaxies is uncertain. Recent observation of 4 low redshift starburst galaxies (Leitherer *et al.* 1995) allows one to get only upper limits of 57%, 5.2%, 11.3%, and 3.2% on the escape fraction (Hurwitz *et al.* 1997). Other arguments based on H $\alpha$  luminosity density of the universe give a more stringent upper limit of  $\sim 1\%$  on the escape fraction (Deharveng *et al.* 1997). We note that our simple assumption, without puncturing, already gives an average escape fraction of 0.4–1% at small redshifts, which is within the observational uncertainties. Therefore, this effect seems unlikely to be more than a few percents at low redshift. However, at high- $z$ , as the star formation rate is higher, it might well be that the puncturing effect allows a larger fraction of ionizing photons to escape.

Throughout this paper we assumed that the damped Lyman- $\alpha$  systems are progenitors of present day galaxies. This assumption has recently been questioned by Prochaska

and Wolfe (1997). They studied the kinematical properties of damped Lyman- $\alpha$  systems at high redshift and concluded that most damped Lyman- $\alpha$  systems correspond to thick rotating disks with rotational velocities  $\simeq 225 \text{ km s}^{-1}$ . We compare these results with the predication of our model. We notice that for standard CDM model, even though about ten percent of the objects have rotational velocities beyond the value of  $\simeq 225 \text{ km s}^{-1}$ , the average rotational velocity of damped Lyman- $\alpha$  systems is  $120 \text{ km s}^{-1}$  at  $z \simeq 3$ , which is too small to be consistent with Prochaska and Wolfe's results. However, this discrepancy is not serious for various reasons. First, the relationship between rotational velocity and  $N_{HI}$  depends sensitively on the cosmology. We tried a structure formation model with an open universe which has  $\Omega = 0.3$ . In this case, the average rotational velocity increases to  $160 \text{ km s}^{-1}$  with more than one fourth of the objects with velocities greater than  $\simeq 225 \text{ km s}^{-1}$ . This increase is not unexpected because in open universes structures of galaxy sizes collapse at higher redshifts as compared to flat cosmology. Second, the distribution of rotational velocities for damped Lyman- $\alpha$  systems depends crucially on the feedback. An increase in feedback parameter  $V_{hot}$  results in an increase in the average rotational velocity by cutting off contributions from smaller systems. Such an increase in the feedback might come from either local uncertainties in feedback (Eq. (2)) or from a global process like a hot IGM with temperature  $T \simeq 10^6 \text{ K}$  at high redshifts and therefore would depend on the thermal history of the IGM. We also compare the distribution of impact parameters in our models with the inference of Prochaska and Wolfe and found good agreement for both cosmogonies. Also, other recent analyses suggest that the evidence of damped Lyman- $\alpha$  systems being thick rotating disk is not compelling (Ledoux *et al.* 1997a, Ledoux *et al.* 1997b.). Ledoux *et al.* studied the kinematical properties of a sample with 26 damped Lyman- $\alpha$  systems and concluded that whereas the velocities upto  $120 \text{ km sec}^{-1}$  might correspond to rotations of individual systems, higher velocities probably involve more than one component (Ledoux *et al.* 1997a, Ledoux *et al.* 1997b.). A similar conclusion, based on simulations, was reached by Haehnelt *et al.* 1997. Therefore, it seems that though the recent studies have thrown light on the nature of damped Lyman- $\alpha$  systems at high- $z$ , it is still too early to draw firm conclusions. However, should it turn out that damped Lyman- $\alpha$  systems at high  $z$  correspond to merging protogalactic HI clumps rather than rotating disk, our conclusions about the HI absorption inside the ISM of a high- $z$  galaxy and consequently the Hydrogen-ionizing flux will be significantly weakened in the sense that it will be more difficult to support the view that sites where a high HI column density is detected also correspond to star forming regions.

## 5 CONCLUSION

We estimated the contribution of star-forming galaxies to the background Lyman-limit flux taking into account the HI and dust absorption in the ISM of individual galaxies in a self-consistent way with the cosmic star-formation history. We assumed that DLA systems correspond to star-forming regions at high-redshift. We conclude that while star-forming galaxies are unlikely to dominate the back-

ground hydrogen-ionizing flux at high redshift, they are most likely to do so in the present universe. The current uncertainties of modelling do not allow us to calculate the redshift of cross-over from quasar-dominated to galaxy-dominated background flux. As already discussed, a good discriminator between these two sources of ionizing-background is the softness of their spectra. Future high-resolution observations of metals (e.g. Carbon) in their various ionization states in the low-column density Lyman- $\alpha$  clouds for  $0 \simeq z \leq 4$  might enable one to find the transition from quasar-dominated to galaxy-dominated background flux.

**Acknowledgements.** We are pleased to thank Patrick Petitjean, R. Srianand and the anonymous referee for pertinent comments on the kinematics of DLAs.

## REFERENCES

Andreani, P. & Franceschini, A. 1996, MNRAS, 283, 85

Bahcall, J. N., et al. 1993, ApJS, 87, 1

Bajtlik, S., Duncan, R. C., & Ostriker, J. P. 1988, ApJ, 327, 570

Bardeen, J.M., Bond, J.R., Kaiser, N., Szalay, A.S. 1986, Ap.J., 304, 15

Bechtold, J., Weymann, R. J., Lin, Z., & Malkan, M. A. 1987, ApJ, 315, 180

Bechtold, J. 1994, ApJS, 91, 1

Blanchard, A., Valls-Gabaud, D., Mamon, G., 1992, A&A, 264, 365

Cen, R. 1992, ApJS, 78, 341

Cole, S., Aragón-Salamanca, A., Frenk, C.S., Navarro, J.F., Zepf, S.E. 1994., MNRAS, 271, 781

Connolly, A.J., Szalay, A.S., Dickinson, M., SubbaRao, M.U., Brunner, R.J., 1997, astro-ph/9706255

Cooke, A. J., Espey, B., & Carswell, R. F. 1997, MNRAS, 284, 552

Davidsen, A. F., Kriss, G. A., & Zheng, W. 1996, Nature, 380, 47

Deharveng, J. -M., Faïsse, S., Milliard, B., & Le Brun V. 1997, astro-ph/9704146

Dekel, A., Silk, J., 1986, ApJ, 303, 39

Désert, F.X., Boulanger, F., Puget, J.L. 1990, A&A, 237, 215

Devriendt, J.E.G., Sadat, R., Guiderdoni, B., 1998, in preparation

Dickey, J. & Garwood, E. 1990, ApJ, 341, 201

Dove, J. B. & Shull, M. 1994, ApJ, 430, 222

Dwek, E., Városi, F., 1996, in *Unveiling the Cosmic Infrared Background*, E. Dwek (ed), AIP Conference Proceedings 348

Efstathiou, G., 1992, MNRAS, 256, 43P

Fall, S.M., Efstathiou, G., 1980, MNRAS, 193, 189

Fall, S.M., Charlot, S., Pei, Y.C., 1996, ApJ, 464, L43

Franceschini, A., Toffolatti, L., Mazzei, P., Danese, L., & De Zotti, G., 1991, ApJSS, 89, 285

Franceschini, A., Mazzei, P., De Zotti, G., Danese, L. 1994, ApJ, 427, 140

Franceschini, A., Andreani, P. 1995, ApJ, 440, L5

Giallongo, E., et al. 1994, ApJ, 425, L1

Giallongo, E., Cristiani, S., D'Odorico, S., Fontana, A., Savaglio, S. 1996, ApJ, 466, 46

Giallongo, E., Fontana, A. & Madau, P. 1997, MNRAS, 289, 629

Giroux, M. L., & Shapiro, P. 1996, ApJS, 102, 191

Guiderdoni, B., Rocca-Volmerange, B. 1987, A&A, 186, 1

Guiderdoni, B., Bouchet, F.R., Puget, J.L., Lagache, G., Hivon, E., 1997a, Nat., 390, 257

Guiderdoni, B., Hivon, E., Bouchet, F.R., Maffei, B., 1997b, MNRAS in press (GHBM)

Gunn, J.E. & Peterson, B.A. 1965, ApJ, 142, 1633

Haehnelt, M.G., Steinmetz, M., Rauch, M., 1997, astro-ph/9706201

Haardt, F., & Madau, P. 1996, ApJ, 461, 20

Heyl, J., Cole, S., Frenk, C. S., Navarro, J. F 1995, MNRAS, 274, 755

Hurwitz, M., Jelinsky, P., & Van Dyke Dixon, W. 1997, astro-ph/9703041

Kauffmann, G.A.M., 1996, MNRAS, 281, 487

Kauffmann, G.A.M., White, S.D.M., Guiderdoni, B., 1993, MNRAS, 264, 201

Kennicutt, R.C., 1989, ApJ, 344, 685

Kennicutt, R.C., Tamblyn, P., Congdon, C.W., 1994, ApJ, 435, 22

Kennicutt, R.C., 1997, in *Starbursts: Triggers, Nature and Evolution*, B. Guiderdoni and A. Kembhavi (eds.), Editions de Physique /Springer–Verlag

Kulkarni, V. P. & Fall, S. M. 1993, ApJ, 413, L63

Lacey, C., Silk, J., 1991, ApJ, 381, 14

Lacey, C., Guiderdoni, B., Rocca-Volmerange, B., Silk, J., 1993, ApJ, 402, 15

Ledoux, C., Petitjean, P., Bergeron, J., Wampler, E. J. & Srianand, R., 1998, submitted for publication

Ledoux, C. Petitjean, P. & Bergeron, J., 1997, to appear in *Structure and Evolution of the Intergalactic Medium from QSO absorption Line Systems*, IAP, Paris

Lilly, S.J., Tresse, L., Hammer, F., Crampton, D., Le Fèvre, O., 1995, ApJ, 455, 108

Lilly, S.J., Le Fèvre, O., Hammer, F., Crampton, D., 1996, ApJ, 460, L1

Lobo, C. & Guiderdoni, B. 1998, in preparation

Madau, P., Ferguson, H.C., Dickinson, M.E., Giavalisco, M., Stein, C.C., Fruchter, A., 1996, MNRAS, 283, 1388

Maffei, B. 1994, PhD Dissertation, Université Paris VII

Maloney, P. 1993, ApJ, 414, 41

Marzke, R.O., Huchra, J.P., Geller, M.J., 1994, ApJ, 428, 43

Mathis, J.S., Mezger, P.G., Panagia, N., 1983, A&A, 128, 212

Miralda-Escudé, J., Cen, R., Ostriker, J. P. & Rauch, M. 1996, ApJ, 471, 582

Miralda-Escudé, J. & Ostriker, J.P. 1992 ApJ, 392, 15

Miralda-Escudé, J. & Ostriker, J. P. 1990, ApJ, 350, 1

Mo, H. J., Mao, S., White, S. D. M. 1997, astro-ph/9707093

Natarajan, P., Pettini, M., 1997, astro-ph/9709014

Paresce, F., McKee, C. F., & Bowyer, S 1980, ApJ, 240, 387

Pei, Y. C. 1995, ApJ, 438, 623

Pei, Y.C., Fall, S.M., 1995, ApJ, 454, 69

Pettini, M., Smith, L.J., King, D.L., Hunstead, R.W., 1997, astro-ph/9704102

Prochaska, J., Wolfe, A., 1997, ApJ in press

Puget, J.L., Abergel, A., Boulanger, F., Bernard, J.P., Burton, W.B., et al., 1996, A&A, 308, L5

Reynold, R. J. 1984, ApJ, 282, 191

Reynolds, R. J., et al. 1995, ApJ, 448, 715

Sanders, D. B., & Mirabel, I. F. 1996, ARAA, 34, 749

Saunders, W., Rowan-Robinson, M., Lawrence, A., Efstathiou, G., Kaiser, N., Ellis, R.S., Frenk, C.S., 1990, MNRAS, 242, 318

Sawicki, M.J., Lin, H., Yee, H.K.C., 1997, AJ, 113, 1

Sethi, S. & B. B. Nath 1997, MNRAS, 289, 634

Soifer, B.T., Neugebauer, G., 1991, AJ, 101, 354

Songaila, A. Cowie, L. L., & Lilly, S. J 1990, ApJ, 348, 371

Songaila, A., & Cowie, L. L. 1996, AJ, 112, 335

Steidel, C.C., Giavalisco, M., Pettini, M., Dickinson, M., Adelberger, K.L., 1996, ApJ, 462, L17

Stengler-Larreaa, E. A., et al. 1995, ApJ, 444, 64

Storrie-Lombardi, L.J., McMahon, R.G., Irwin, M.J., 1996, MNRAS, 283, L79

Vogel, S., Weymann, R., Rauch, M., & Hamilton, T. 1995, ApJ, 441, 162

Zhang, Y., Anninos, P., Norman, M. L., & Meiksin, A. 1996,  
astro-ph/9609194

Zwaan, M. A., Briggs, F. H., Sprayberry, D., & Sorar, E., ApJ in  
press

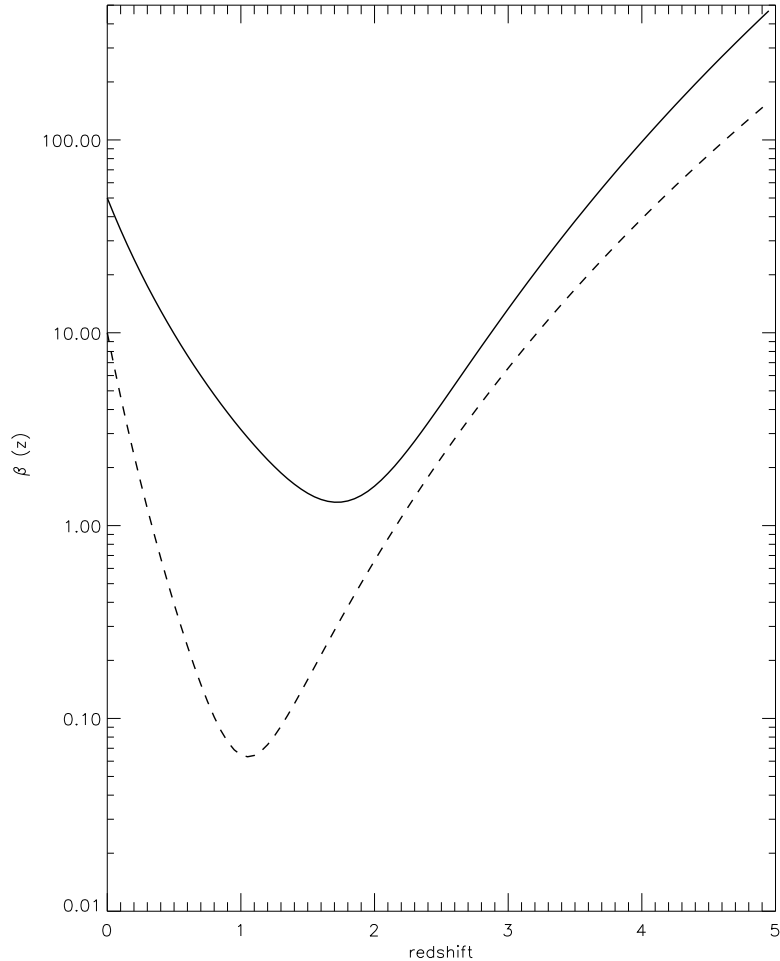


**Figure 1.** Efficiency parameter evolution with redshift. The *thick solid* and *dashed* lines show the values used for model I and II respectively. Analytical expressions for  $\beta(z)$  are  $\beta(z) = 50(1 + 10^{-6}(1 + z_{coll})^{13})/(1 + z_{coll})^4$  (model I) and  $\beta(z) = 10(1 + 10^{-5}(1 + z_{coll})^{16})/(1 + z_{coll})^8$  (model II).

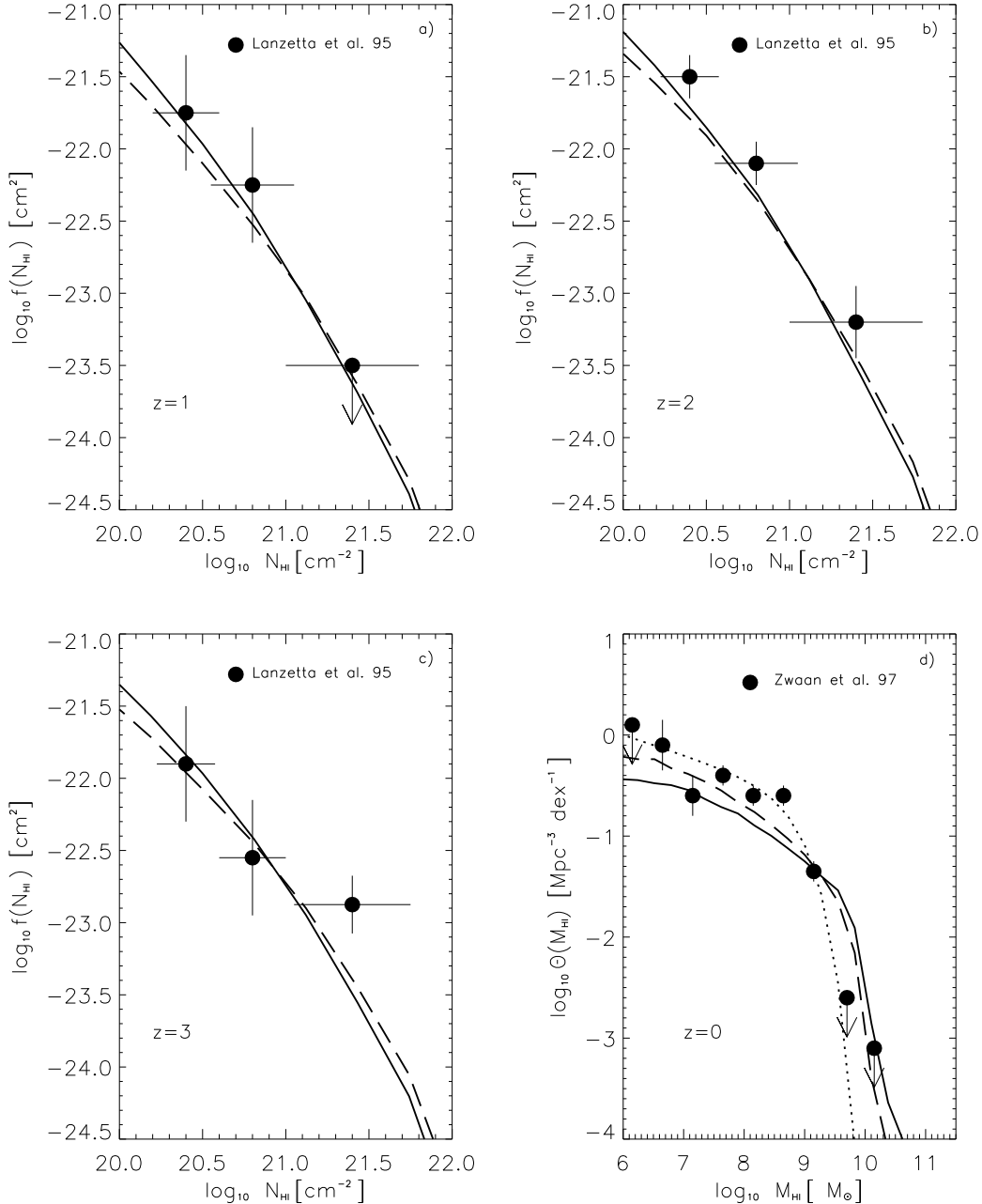


**Figure 2.** Fig. 2a: Distribution of damped Lyman- $\alpha$  absorbers as a function of their HI column density at  $z \simeq 1$ . Thick solid and long-dashed lines are respectively the predictions of models I and II. Fig. 2b: Same as panel a) for  $z \simeq 2$ . Fig. 2c: Same as panel a) for  $z \simeq 3$ . Fig. 2d: HI mass function of galaxies at  $z \simeq 0$ . Thick solid, long dashed, and dotted curves are respectively models I and II predictions and a Schechter fit to the data given by Zwaan et al. 97.

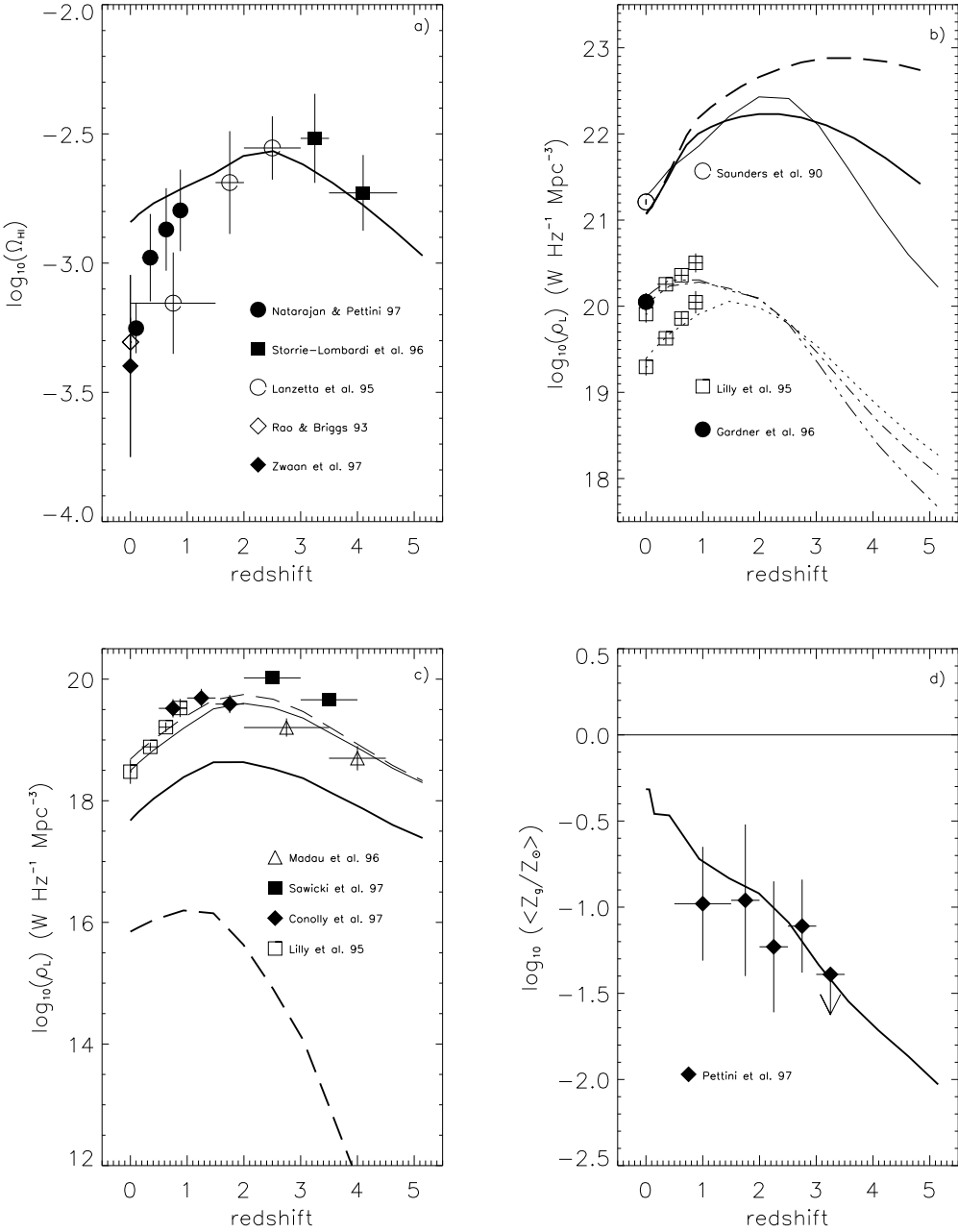


**Figure 3.** Fig. 3a: Evolution of the cold gas density parameter in DLA absorbers. The fit from Model I is indicated by the *thick solid* line. Fig. 3b: Rest-frame comoving luminosity density from optical to FIR. The *thin dotted*, *dot-dashed*, *triple-dot-dashed* and *solid* lines respectively stand for emissivities at 4400 Å, 10000 Å, 22000 Å and 60 μm given by model I. Open squares: local and Canada-France Redshift Survey (Lilly et al. 96). Open circle: 60 μm local density corresponding to one third of the bolometric light radiated in the IR (Saunders et al. 90). Solid circle: 2.2 μm local luminosity density (Gardner et al. 96). The *thick solid* and *dashed* lines are respectively models (A) and (E) from GHBM that give reasonable fits of the CIB. Fig. 3c : Rest-frame comoving luminosity density from far-UV to UV. The *thin solid* and *long-dashed* lines, represent emissivities at 1620 Å and 2800 Å given by model I. The *thick solid* and *long-dashed* lines are predictions of the same model for luminosity at 912 Å respectively without and with HI absorption, but with dust absorption. Solid diamonds: photometric redshifts in the Hubble Deep Field (Connolly et al. 97) taking into account NIR data. Solid squares: other estimates of photometric redshifts in the HDF (Sawicki et al. 97). Open triangles: HDF with redshifts from Lyman-continuum drop-outs (Madau et al. 96). Fig. 3d : Evolution of the mean metallicity in damped Lyman-α absorbers. Prediction from Model I is indicated by the *thick solid* line. Since the chemical evolution model is a closed-box one, the metallicity of the systems is certainly overestimated if a fraction of the metals is ejected in the IGM.

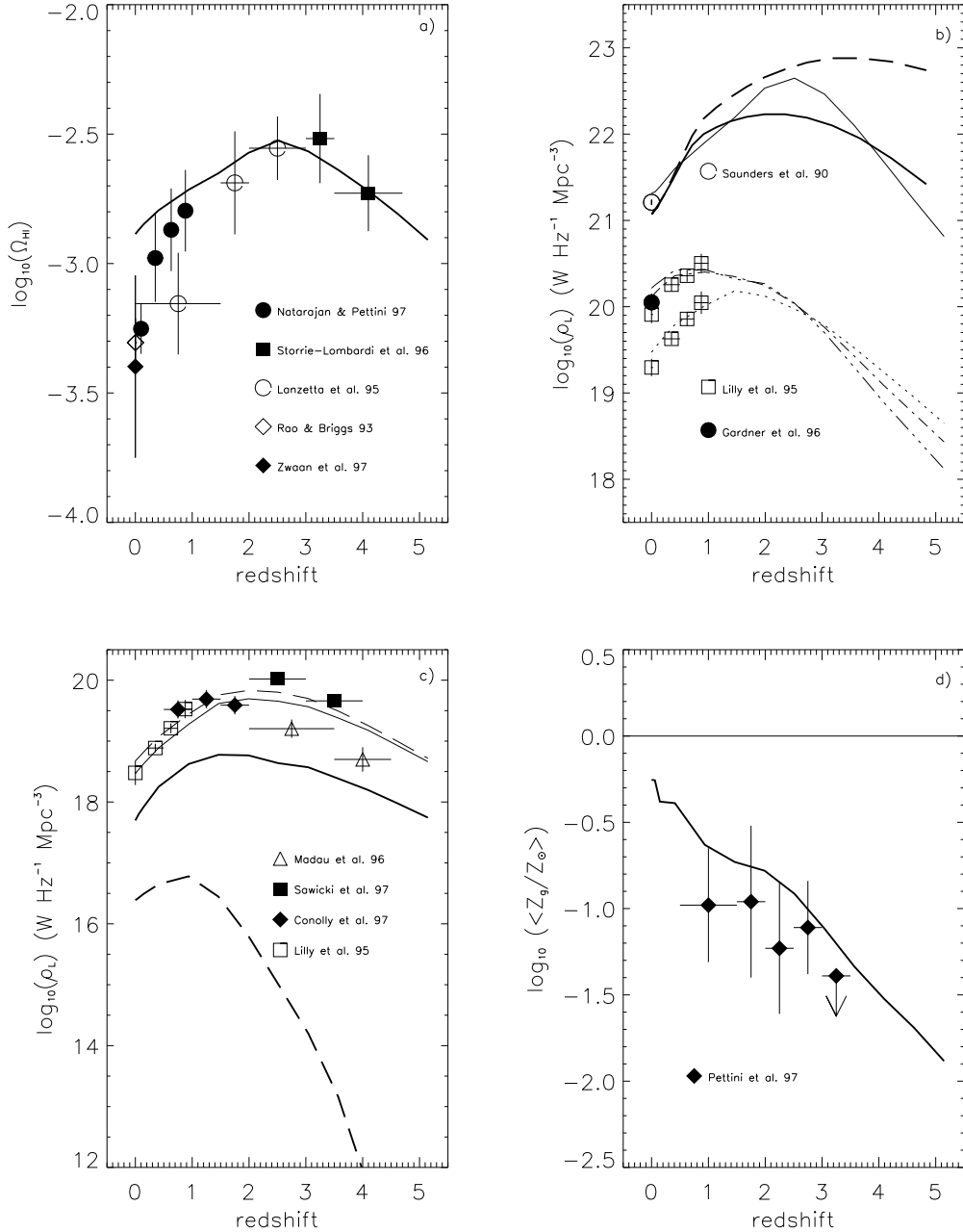
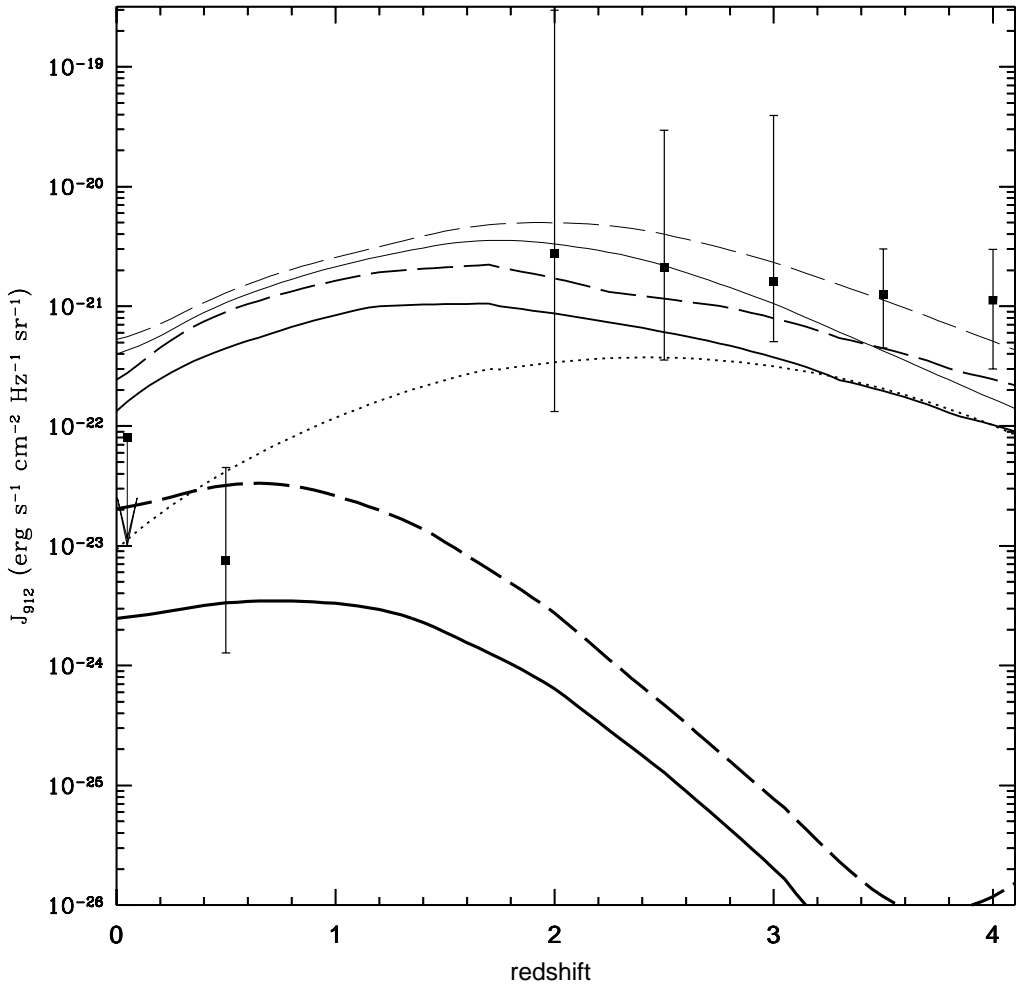


Figure 4. Same as Fig. 3 for model II.



**Figure 5.** The evolution of Lyman-limit flux is shown for the various cases discussed in the text. The *solid* lines give the predictions of Model I. The lines of increasing thickness correspond respectively to models without dust and HI absorption, with dust but without HI absorption, and with both dust and HI absorption. The *dashed* lines are the corresponding predictions of Model II. The *dotted* line shows the evolution of background Lyman-limit flux from quasars. The upper limit at  $z \simeq 0$  is from Vogel et al. (1995), the data point at  $z \simeq 0.5$  is from Kulkarni and Fall (1993), the high redshift data points are from Cooke et al. (1997).